INVESTIGATION OF THE THERMAL MIXING IN A T-JUNCTION FLOW WITH DIFFERENT SRS APPROACHES

M. S. Gritskevich[1], A. V. Garbaruk[1], Th. Frank[2] and F. R. Menter[2]

[1]St. Petersburg State Polytechnical University, 195251, St. Petersburg, Russia
[2]Software Development Department, ANSYS, 83714, Otterfing, Germany

e-mail: Florian. Menter@ansys.com

Abstract

An investigation of different turbulence Scale-Resolving Simulation (SRS) modeling approaches for the flow in a T-junction has been conducted using the Scale-Adaptive Simulation (SAS), the Delayed Detached Eddy Simulation (DDES) and the Embedded Large Eddy Simulation (ELES) methods. The results show that all models are able to accurately predict the mean and RMS velocity profiles, when used in combination with a low dissipation advection scheme. However, when a slightly more dissipative scheme is used, the SAS model yields less accurate results, indicating that this flow does not produce a strong enough flow instability to allow the safe application of this model. The DDES and the ELES models show less sensitivity to the numerical setting compared to the SAS model. The main goal of the study is the accurate prediction of heat transfer on the walls in the mixing zone. In that respect, the ELES method produces the most consistent agreement with the experimental data.

1. INTRODUCTION

Turbulent mixing of fluids of different temperatures in T-junction geometries is of significant importance in the field of nuclear reactor safety, since it can lead to highly transient, low frequency temperature fluctuations on the adjacent pipe walls, to cyclic thermal stresses in the pipe walls and consequently to thermal fatigue and failure of the piping. The unsteady thermal mixing of two fluid streams of different temperature as well as the accurate prediction of the velocity field is a challenging test for Computational Fluid Dynamics (CFD). CFD methods based on Unsteady Reynolds Averaged Navier-Stokes (URANS) formulations, which are typically used in industrial applications, have difficulties in providing accurate results for such flows. In many cases, the high turbulent viscosity predicted by the RANS models in the mixing zone due to the locally high shear rates suppresses any transient flow development and the CFD results converge to a steady-state solution. On the other hand, experimental observations clearly show strong temperature transients on the pipe walls downstream of the T-junction (the so-called thermal striping effect). Recent studies using advanced Scale-Resolving Simulation (SRS) models such as Large Eddy Simulation (LES), Detached Eddy Simulation (DES) (Spalart 2009; Spalart et al. 1997; M. Strelets 2001) and Scale-Adaptive Simulation (SAS) (F. R. Menter & Kuntz 2004; Egorov et al. 2010; F. R. Menter & Egorov 2010) have shown promising results (Ohtsuka et al. 2003; Igarashi et al. 2003; Hu & Kazimi 2003; Braillard et al. 2005; Frank et al. 2010). However, a detailed validation of such methods is still required in order to determine their range of validity and their accuracy.

For that purpose, a recently proposed OECD benchmark test case (OECD/NEA 2011; OECD/NEA 2009; Mahaffy 2010) is investigated. The corresponding experiment was carried out by Vattenfall in 2009 at the Älvkarleby Laboratory (Odemark et al. 2009), Vattenfall Research and Development AB.

In the present report, several SRS approaches are considered, namely Delayed Detached Eddy Simulation (DDES) (Spalart et al. 2006), SAS (F. R. Menter & Egorov 2010) and Embedded Large Eddy Simulation (ELES) (Davor Cokljat et al. 2009) in combination with an algebraic Wall Modeled LES (WMLES) formulation (Shur et al. 2008). The simulations are based on ANSYS Fluent 13.0. All turbulence models are tested with the use of two different advection interpolation schemes, namely Central Difference (CD) and Bounded Central Difference (BCD) (Jasak et al. 1999), since the stability of the flow in the T-Junction test case can be strongly influenced by the dissipative properties of the numerical scheme of the CFD code.

2. TEST CASE DESCRIPTION

The model tests were carried out in 2009 at the Älvkarleby Laboratory, Vattenfall Research and Development (Odemark et al. 2009). The related test case conditions had been documented in the OECD benchmark specification (OECD/NEA 2011; OECD/NEA 2009; Mahaffy 2010). The test rig is illustrated in Fig. 1.

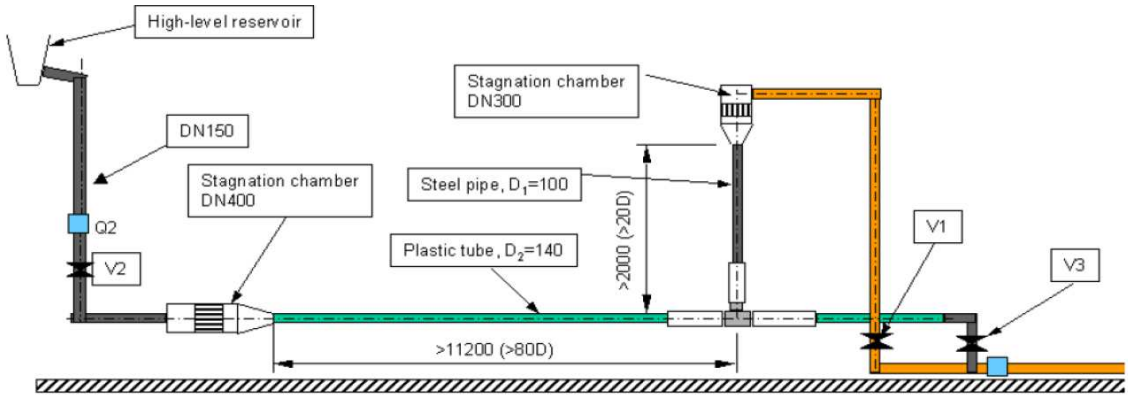

Fig. 1. Side view of the Vattenfall T-junction test facility in the vertical plane (dimensions are given in mm)

The setup consists of a vertical pipe with inner diameter D_v and a horizontal pipe with an inner diameter D_h with a diameter ratio of D_h/D_v=1.4. The length of the straight pipes upstream of the T-junction is more than $80D_h$ for the horizontal pipe, and approximately $20D_v$ for the vertical pipe. All the experimental tests were carried out with water. The mass flow ratio in the two pipes was kept constant throughout the experiment (Q_h/Q_v=1.5). The Reynolds number based on bulk velocity and pipe diameter were approximately $Re_v=\rho \cdot U_{b,v} \cdot D_v/\mu_v=8 \cdot 10^4$ and $Re_h=\rho \cdot U_{b,h} \cdot D_h/\mu_h=1 \cdot 10^5$ for vertical and horizontal pipes respectively. The temperature of the water was T_v=309 K and T_h=292 K in the vertical and horizontal pipes respectively with a temperature difference of ΔT=17 K. The Prandtl number was different for each pipe with $Pr_v=\mu_v \cdot C_p/\lambda \approx 5$ and $Pr_h=\mu_h \cdot C_p/\lambda \approx 7$ in the vertical and horizontal pipes respectively. In the current simulations, density, specific heat capacity, and thermal conductivity are assumed to be constant, while the dynamic viscosity is modeled with the use of piecewise polynomial approximation based on the data from (OECD/NEA 2009; OECD/NEA 2011; Mahaffy 2010).

3. NUMERICAL SET-UP

A sketch of the domain is shown in Fig. 2. The inlet section is located at Z/D_v=3.1 and at X/D_h=-3.0 in the vertical and horizontal pipe respectively. The outlet section is located at X/D_h=20.0. When ELES is used, the inlet RANS-LES interface is located at Z/D_v=-0.7 and at X/D_h=-1.0 in the vertical and horizontal pipe respectively, while the outlet RANS-LES interface is located at X/D_h=7.0.

The computational grid for this flow consists of about 4.9 million hexahedral cells (see Fig. 2). The grid size in wall normal direction is set to have $\Delta y^+<1$ in most of the domain. The grid step in axial and circumferential direction is chosen as follows. For the horizontal pipe, the grid has $\delta_h/\Delta_{axial} \approx 20$ and $\delta_h/\Delta_{circumferrential} \approx 33$, where $\delta_h=0.5D_h$ is the boundary layer thickness at the horizontal pipe inlet section (the flow is fully developed). For the vertical pipe the grid has $\delta_v/\Delta_{axial} \approx 6$ and $\delta_v/\Delta_{circumferrential} \approx 15$, where $\delta_v=0.22D_v$ is the boundary layer thickness at the vertical pipe inlet section. In wall units, the grid parameters are $(\Delta_{axial}^+, \Delta_{circumferrential}^+) \approx (7500, 3000)$ for the vertical pipe and $(\Delta_{axial}^+, \Delta_{circumferrential}^+) \approx (7500, 4500)$ for the horizontal pipe, which means that the flow cannot be handled by conventional LES on the current grid. For this reason the different hybrid RANS-LES models listed above have been employed. The time step is equal to $\Delta t=0.016 \cdot D_v/U_b$ which leads to maximum CFL number of around 4 near the junction. To obtain unsteady statistics, the instantaneous flow fields are averaged over 40000 time steps which correspond to approximately 27 convective time units ($23.1 \cdot D_v/U_b$). Averaging has been started after a statistically converged solution was obtained. When starting the simulation from a RANS solution, this requires of the order of 10000 time steps.

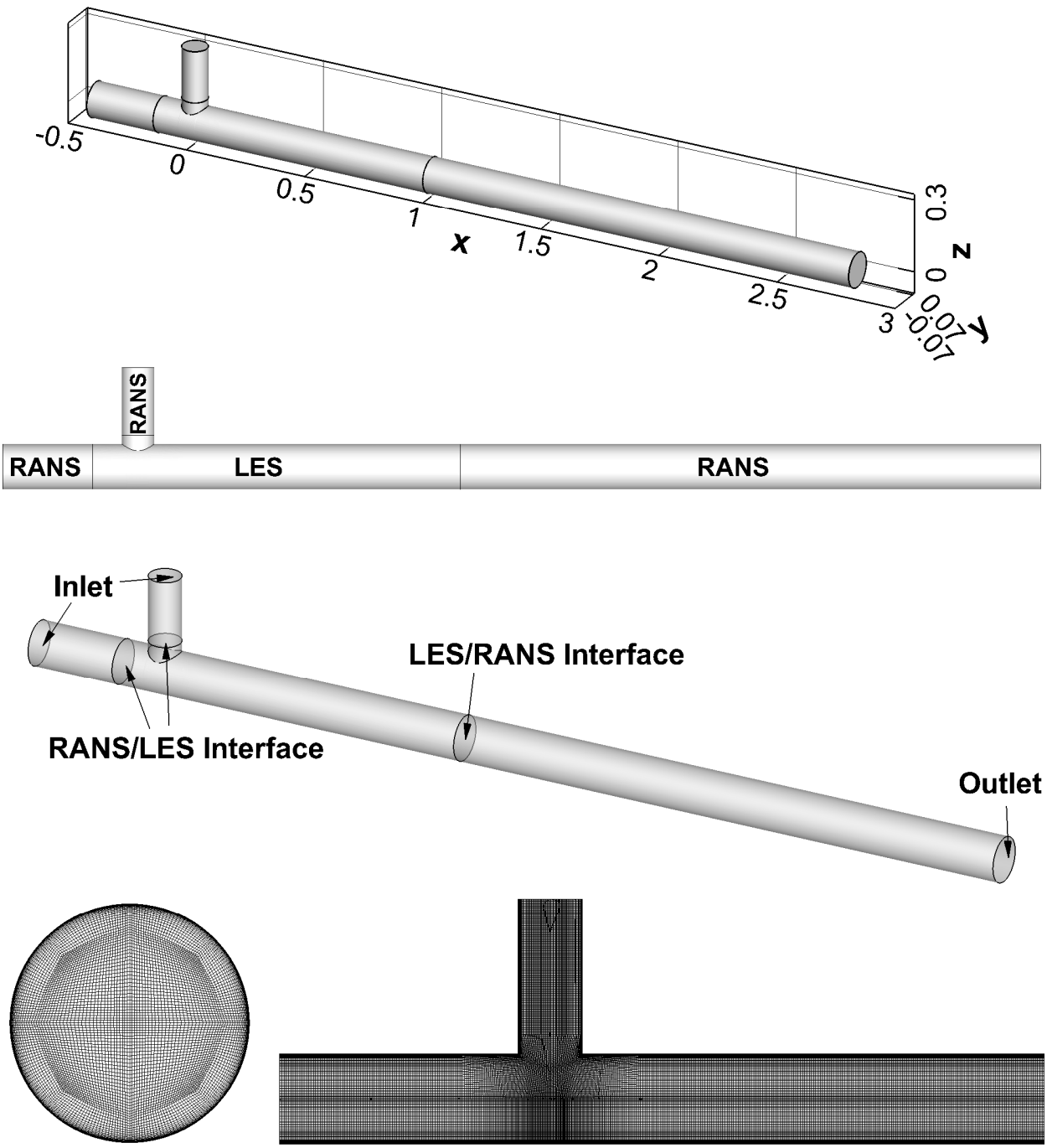

Fig. 2. Computational domain and computational grid for the T-Junction flow (X/D=Y/D=Z/D=0 corresponds to the pipe center lines intersection)

The boundary conditions for this case are specified as follows. For the inlet boundaries, precursor simulations of the pipe flow are performed using the SST RANS model. For the cold leg pipe, fully developed pipe flow is calculated using the SST model and the profiles of velocity, temperature, and turbulence quantities are specified on the inlet boundary. For the hot leg, the pipe flow is calculated to fit the thickness of the experimental profiles and then these extracted profiles are specified on the hot water pipe inlet in the same manner as for the cold water one. This allows the consistent specification not only of the mean flow, but also of the turbulence quantities.

All the simulations within the report have been carried out with the use of the ANSYS Fluent 13.0 CFD code. Within this code, the governing equations are written in a transient formulation and the incompressible fluid assumption is selected. A finite volume method on unstructured grids with a cell-centered data arrangement is adopted. The equations are solved with the use of the implicit point Gauss-

Seidel method using a Rhie-Chow flux correction (Rhie & Chow 1983) which is aimed at suppressing unphysical pressure oscillations. An algebraic multigrid solver is applied for convergence acceleration by computing corrections on a series of grids. The SIMPLEC method (Patankar 1980) is used for pressure-velocity coupling and 10 sub iterations per time step are performed. The inviscid fluxes in the momentum equations are approximated with the use of the second order centered scheme (CD) (Murthy et al. 2006) and with the use of second order bounded central difference scheme (BCD) (Jasak et al. 1999), while in the temperature and the turbulence equations the second order upwind scheme is used (Kim et al. 1998). For pressure interpolation, the "Standard" interpolation (weighted interpolation based on central coefficients) is utilized (Mathur & Murthy 1997) and the gradients are approximated with the use of cell based Green-Gauss theorem (Kim et al. 1998). The time derivatives are approximated with the use of the three-level second order backward Euler scheme (Murthy et al. 2006).

4. DESCRIPTION OF THE FLOW PHYSICS AND MODELING APPROACH

In the current test case, there are numerous physical effects which are of relevance for the CFD simulation. There are different instability mechanisms in the mixing zone resulting from the interaction of the two pipe flows.

One effect is a result of the different sizes of the two pipes. The hot-leg pipe is of smaller diameter than the cold one. As a result, the hot flow has some characteristics of a jet in cross-flow relative to the cold flow in the larger pipe. This can produce phenomena similar to vortex shedding behind a cylinder in cross-flow with a distinct Strouhal frequency. Due to the relatively small mismatch in pipe diameter, this effect is not as pronounced as in a free jet in cross-flow, but it does affect the development of the flow. In the simulations, it is observed that there is a relatively slow variation of the flow field, resulting in the need for fairly long time averages. It is assumed that the lateral motion of the 'jet' emanating from the smaller pipe is the physical effect behind this observation.

Secondly, there is a flow instability in the shear layer emanating from the start of the pipe intersection. This flow phenomenon is similar to Kelvin-Helmholtz instability and is responsible for strong thermal mixing in the most upstream portion of the interaction zone.

Finally, the formation of a horseshoe vortex is observed upstream of the 'jet' injected from the smaller pipe. Again, the 'jet' acts like a cylinder in cross-flow to the flow in the larger pipe. All three flow phenomenon interact in a complex way with each other and with the turbulence from the upstream pipe flows.

Due to the need for resolving the unsteady nature of the flow and especially the unsteady temperature fluctuations on the walls (thermal striping), the simulations have to be carried out in unsteady mode. It is known that the application of standard RANS models in unsteady mode (URANS) is not sufficient for computing such turbulence mixing regimes. It is therefore required to apply SRS models which can resolve the unsteady turbulence in the mixing zone.

When using global models like SAS and DDES, the models will only convert to SRS mode if the instability of the flow is sufficiently strong to generate 'new' turbulence, which then essentially overrides the upstream turbulence from the pipe flows. The current flow is not necessarily in that category, as the length and time scales of the upstream (pipe) turbulence are of the same order as the turbulence scales in the mixing zone. In addition, it is not clear if the flow instabilities described above are of sufficient strength to override the existing turbulence from the pipe flows. The application of global models is therefore running the risk of not switching to full SRS mode in the mixing zone. From this model family, the SAS and the DDES model are investigated. Special emphasis is placed on the formation of resolved turbulence structures and the dependency of such formation processes on the numerical scheme employed in the solver.

In order to avoid this ambiguity of global models, the simulations have also been carried out with an embedded LES (ELES) model, which employs a RANS model in the undisturbed pipe sections and a WMLES formulation starting upstream of the mixing zone. At the RANS-LES interface, modeled turbulence from the upstream RANS region is converted with the use of a Vortex Method (Mathey 2008;

Mathey et al. 2006) into synthetic turbulence. This allows the simulation to account for any interaction of the upstream pipe turbulence with the turbulence generated in the mixing zone. Such simulations do not depend so crucially on the resolution of the initial flow instability for the formation of unsteady structures.

5. RESULTS

Experimental data for this flow are available for several X/D sections (1.6, 2.6, 3.6, and 4.6). These sections are shown in green in Fig. 3. Since the region of interest is near the junction, all the charts are plotted at the X/D=1.6 and X/D=2.6 sections. In these sections, profiles of mean and RMS values of U, V, and W velocities are available in horizontal and vertical planes. To investigate the flow topology, mean velocity and temperature contours are also shown in different sections. To investigate the thermal mixing process, the non-dimensional mean temperature as well as the RMS temperature were plotted along the pipe wall (x-direction) at four lines named as top - 0°, front - 90°, bottom - 180° and rear - 270°.

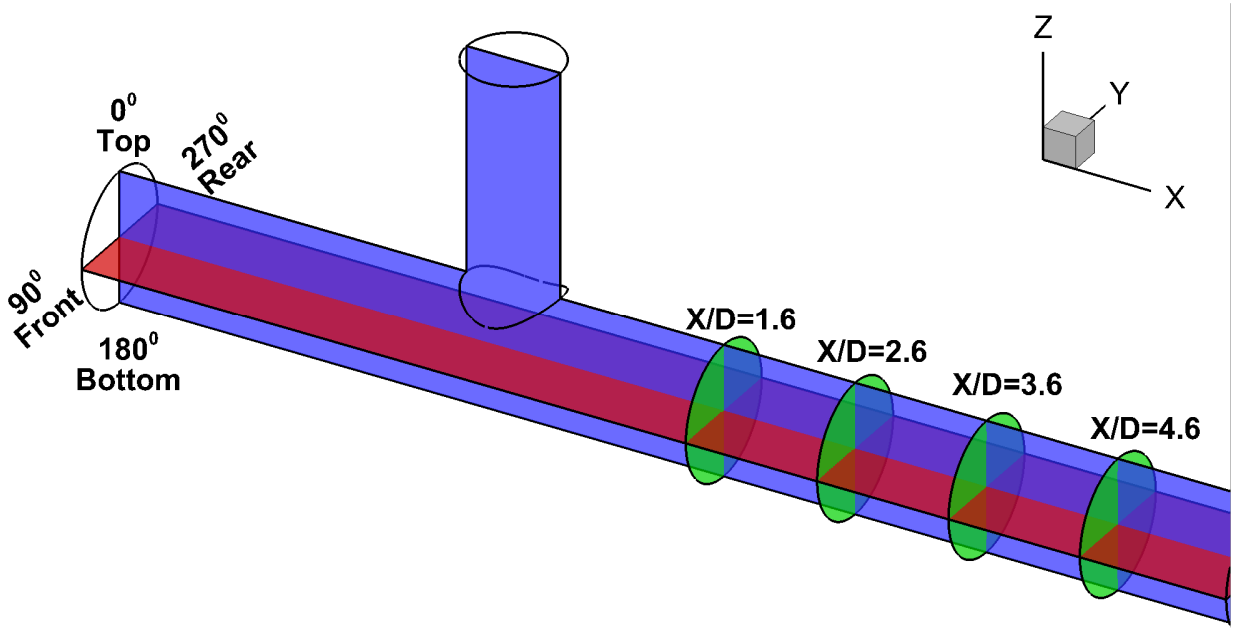

Fig. 3. A sketch of the T-Junction computational domain with the experimental sections

Fig. 4 shows unsteady structures as predicted by the different turbulence models (iso-surfaces of Q=200 s^{-2} colored with velocity contours). The SAS and DDES models show the formation of unsteady turbulence structures emanating from the initial mixing of the two streams. In the mixing zone, 'new' turbulence is formed which then dominates the downstream mixing processes. In the ELES-WMLES simulation, resolved turbulence is already introduced at the RANS-LES interfaces which are then also accounted for in the mixing zone.

As stated already, the application of global models like SAS and DDES can be compromised if the initial instability is not sufficiently strong, and/or if it is suppressed by numerical dissipation. This effect can be seen in Fig. 4 showing SAS simulations using a CD and a BCD scheme. The BCD scheme is more dissipative and thereby inhibits the formation of resolved turbulence in combination with the SAS model. This is an indication that the application of global models to the current application has to be monitored closely, to avoid unphysical results. It is found that the DDES model is less sensitive to numerical settings compared to the SAS model.

Contour plots of the flow in T-Junction can be seen in Fig. 5 and Fig. 6, where velocity and temperature distributions from the ELES-WMLES with the CD scheme are plotted. The hot water is strongly cooled downstream of the junction and at X/D=4.6 the flow in the pipe has nearly constant temperature (however, a small peak can be still observed). The thermal striping phenomenon takes place mostly in the upstream part of the mixing layer, where high values of temperature fluctuations (about $0.3 \cdot \Delta T$) are observed (see RMS temperature contours in Fig. 6). Further downstream, the magnitude of these

fluctuations decreases and at X/D=4.6 it is as low as 0.1·ΔT with a nearly constant distribution across the section.

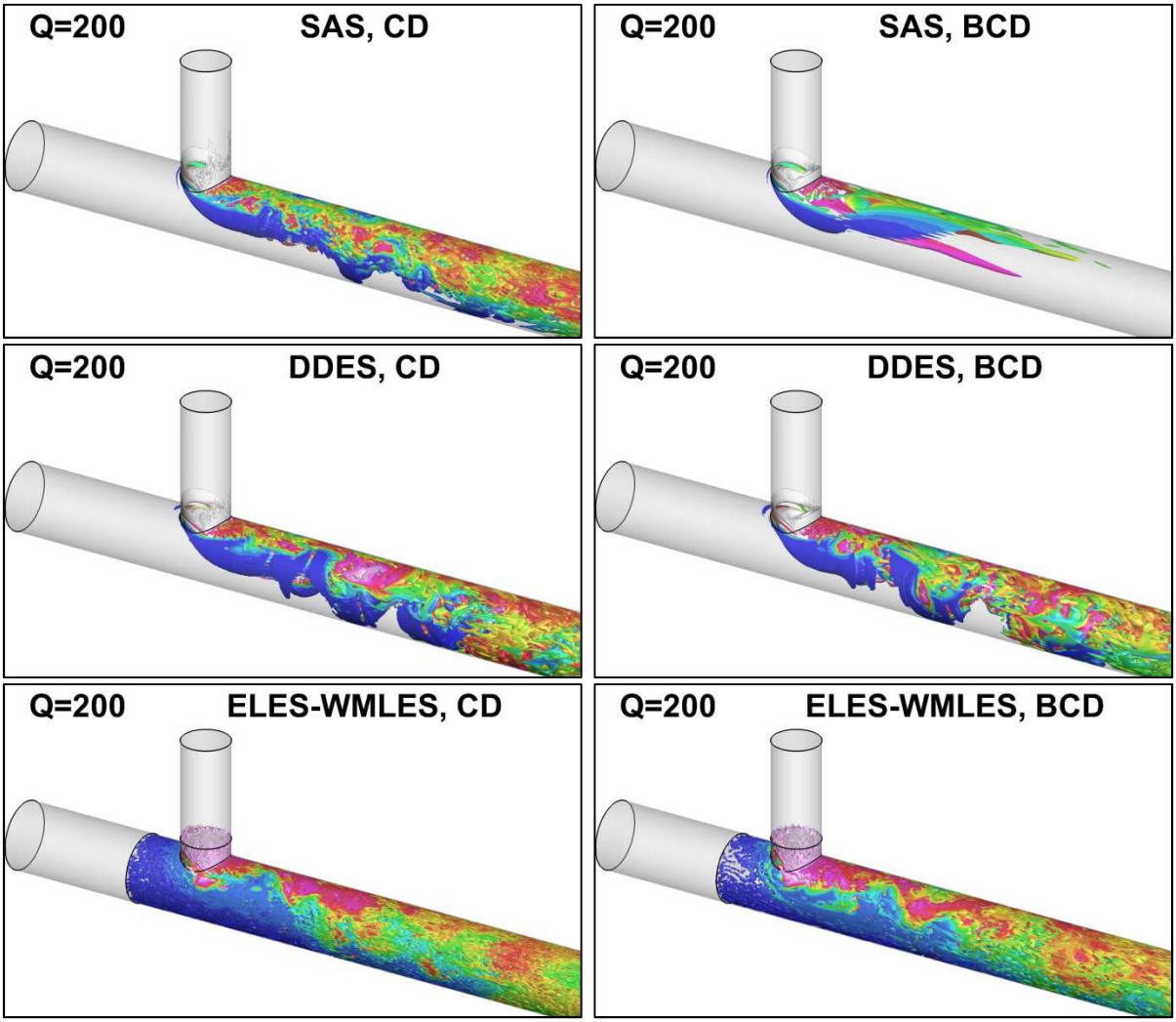

Fig. 4. Isosurfaces of Q-criterion colored with temperature

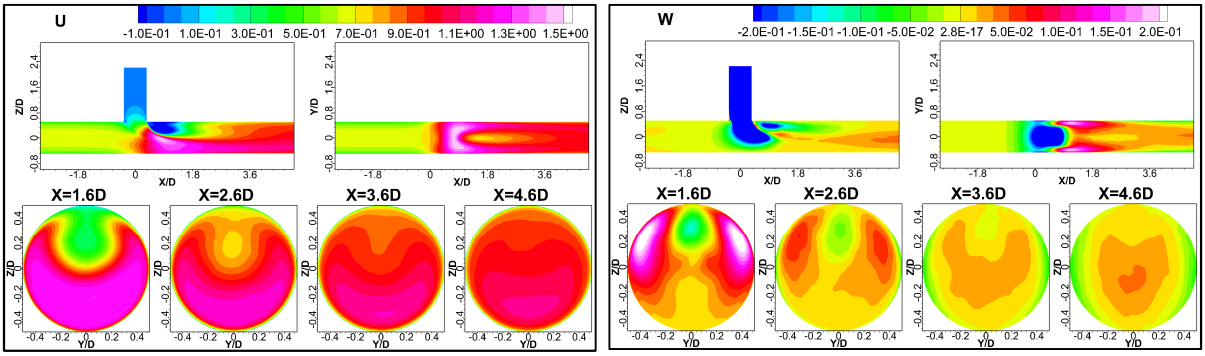

Fig. 5. Mean velocity contours using the ELES-WMLES with CD scheme

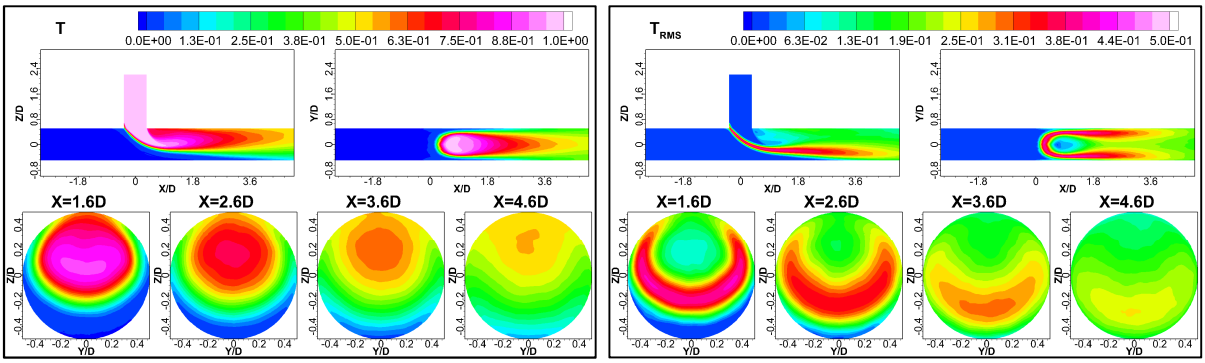

Fig. 6. Mean and RMS temperature contours using the ELES-WMLES with CD scheme

5.1. Velocity Field Predictions

As seen from mean and RMS velocity profiles (see Fig. 7 and Fig. 8) very good agreement between the results and the experimental data is observed and the change of the scheme from CD to BCD does not impair the solution for the DDES and ELES-WMLES approaches. However, when the SAS model is used with the BCD scheme, the mixing layer emanating from the branch pipe downstream the junction remains stable (see Fig. 4) and as it has been already mentioned above, the flow downstream of the junction is then predicted in RANS mode. The lack of the resolved coherent turbulent structures downstream of the junction observed for SAS with BCD results in a significant underestimation of resolved RMS velocities especially for U_{RMS} and V_{RMS}, while the other models agree better with the experimental results. It is worth noting that for all considered approaches, the maximum values of U_{RMS} in vertical sections are about 20% smaller than in the experiment, while near the wall good agreement is achieved. The reason of such differences is yet unknown.

In summary, all models are able to predict the time averaged mean and RMS velocity profiles with good accuracy, when combined with the CD scheme for advection. The SAS model reverts back to URANS mode when used in combination with the BCD scheme.

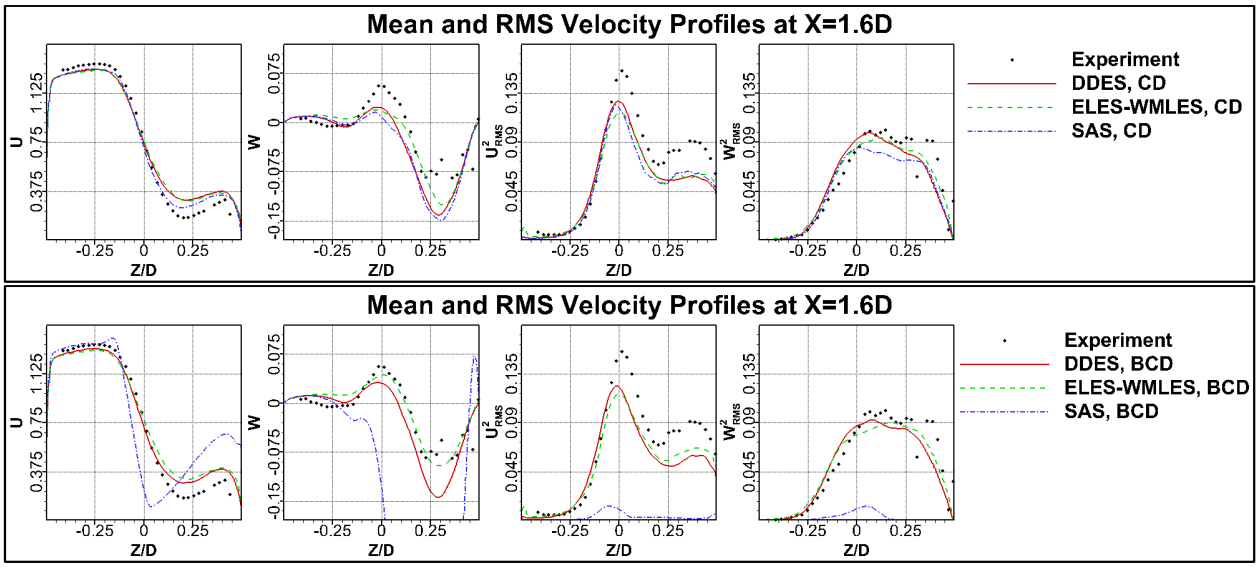

Fig. 7. Mean and RMS velocity profiles at X/D=1.6 in vertical (YZ) section

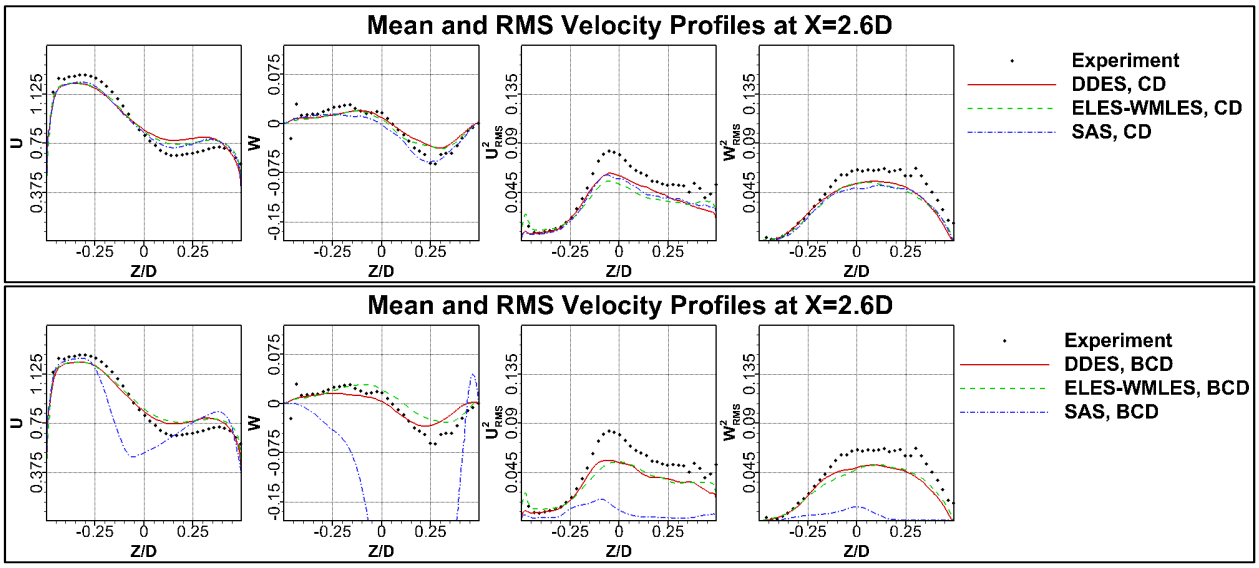

Fig. 8. Mean and RMS velocity profiles at X/D=2.6 in vertical (YZ) section

5.2. Temperature Field Predictions

To analyze the heat transfer predictions, mean and RMS temperature values of the temperature are plotted in Fig. 9 and Fig. 10. The comparison with data is plotted along lines indicated in Fig. 3 as 'Top', 'Front'. 'Bottom' and 'Rear', downstream of the pipe junction. As seen, the best results are obtained with the use of ELES-WMLES approach, for which almost perfect distributions of the wall temperatures are obtained. As it has been already mentioned above, the influence of the numerical scheme (CD, BCD) is marginal for this approach. However, for models for which no resolved turbulent content is specified in the branch and the main pipe upstream of the intersection in (SAS and DDES), the results of the wall temperature are noticeably less accurate than those obtained with the ELES-WMLES approach. The main difference can be seen on the lines on the Top and Bottom parts of the wall, where the temperatures predicted with both DDES and SAS have a spurious minimum near X/D=1 on the Top part of the wall and an underestimation of temperature on the Bottom section. The temperature in the Front and Rear sections are predicted virtually identically with all models, except near the T-junction, where there are however no exp. data available.

Consistently with previous observations for the combination of the SAS model with the BCD scheme, the thermal mixing is predicted incorrectly. As can be seen from Fig. 9, the wall temperature is significantly underestimated in all considered wall sections. It should be noted that similar tendencies, but less severe are also observed for DDES with the BCD scheme.

The results for the RMS temperature shown in Fig. 10 indicate that all models, except SAS-BCD predict RMS temperature fluctuations in good agreement with the data.

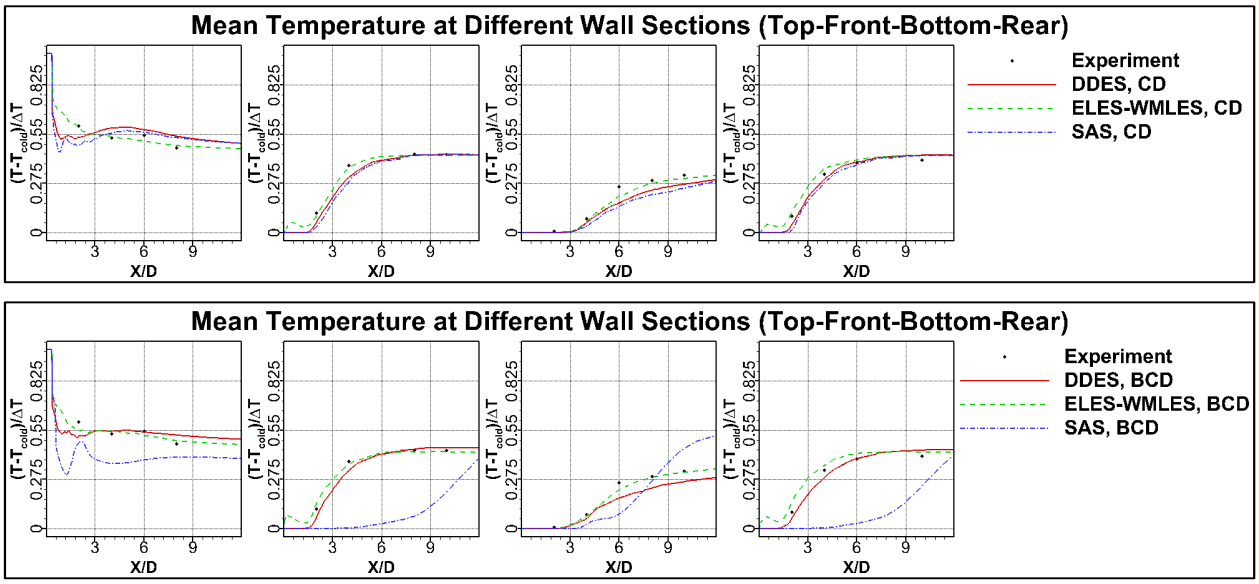

Fig. 9. Mean temperature profiles for different models and numerical schemes

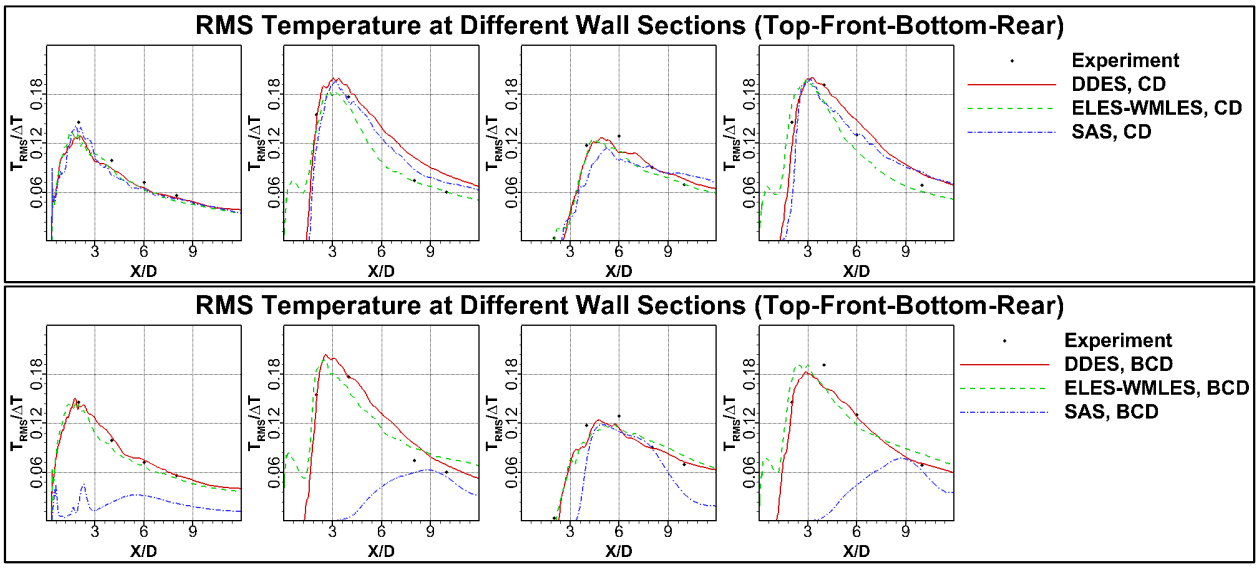

Fig. 10. RMS temperature profiles for different models and numerical schemes

6. SUMMARY

An investigation of different turbulence modeling approaches for the thermal mixing in a T-junction flow has been carried out. The main emphasis is on the comparison of global vs. zonal SRS models.

The results show that all models are able to accurately predict the mean and RMS velocity profiles, when used in combination with a low dissipation CD scheme. The SAS model leads to steady results when combined with a slightly more dissipative BCD scheme, indicating that this flow does not produce a strong enough flow instability to allow application of this model. The DDES model is less sensitive to the numerical setting than SAS, but also misses some of the interactions of the thermal mixing process with the upstream pipe turbulence.

In contrast, ELES with WMLES method yields very good results which do not depend on the advection scheme and therefore this method is more reliable for such type of flows. Very good agreement with the experimental data is obtained with this method. Since the turbulence mixing zone is confined by walls, zonal or embedded LES methods can be applied without much overhead relative to global models. Under such conditions, the use of such models is preferable.

REFERENCES

Braillard, O., Jarny, Y. & Balmigere, G., 2005. Thermal load determination in the mixing Tee impacted by a turbulent flow generated by two fluids at large gap of temperature. *ICONE13-50361, 13th International Conference on Nuclear Engineering, Beijing, China, May 16-20*.

Cokljat, Davor et al., 2009. Embedded LES Methodology for General-Purpose CFD Solvers. *6th International Symposium on Turbulence and Shear Flow Phenomena*, pp.1191-1196.

Egorov, Y. et al., 2010. The Scale-Adaptive Simulation Method for Unsteady Turbulent Flow Predictions. Part 2: Application to Complex Flows. *Flow Turbulence and Combustion*, 85(1), pp.139-165.

Frank, T. et al., 2010. Simulation of turbulent and thermal mixing in T-junctions using URANS and scale-resolving turbulence models in ANSYS CFX. *Nuclear Engineering and Design*, 240(9), pp.2313-2328.

Hu, L.-W. & Kazimi, M.S., 2003. Large Eddy Simulation of Water Coolant Thermal Striping in a Mixing Tee Junction. *The 10th Int. Topical Meeting in Nuclear Reactor Thermal Hydraulics (NURETH-10), Seoul, Korea, October 5-9*, pp.1-10.

Igarashi, M. et al., 2003. Study on Fluid Mixing Phenomena for Evaluation of Thermal Striping in a mixing Tee. *The 10th Int. Topical Meeting in Nuclear Reactor Thermal Hydraulics (NURETH-10), Seoul, Korea, October 5-9*, pp.1-12.

Jasak, H., Weller, H.G. & Gosman, A.D., 1999. High resolution NVD differencing scheme for arbitrarily unstructured meshes. *Int. J. Numer. Meth. Fluids*, 31, pp.431–449.

Kim, S.E., 2004. Large eddy simulation using an unstructured mesh based finite-volume solver. *AIAA Paper*, 2004-2548.

Kim, S.E. et al., 1998. A reynolds averaged Navier-Stokes solver using unstructured mesh-based finite-volume scheme. *AIAA Paper*, 98–0231.

Mahaffy, J., 2010. Synthesis of Results for the T-Junction Benchmark. In *CFD4NRS-3 Conference on Experimental Validation of CFD and CMFD Codes to Nuclear Reactor Safety Issues*. Washington, DC, USA, p. 3.

Mathey, F., 2008. Aerodynamic noise simulation of the flow past an airfoil trailing-edge using a hybrid zonal RANS-LES. *Computers & Fluids*, 37, pp.836–843.

Mathey, F. et al., 2006. Assessment of the vortex method for Large Eddy Simulation inlet conditions. *Progress in Computational Fluid Dynamics*, 6, pp.58-67.

Mathur, S.R. & Murthy, J.Y., 1997. A pressure-based method for unstructured meshes. *Numerical Heat Transfer*, 32, pp.195–215.

Menter, F.R. & Egorov, Y., 2010. The Scale-Adaptive Simulation Method for Unsteady Turbulent Flow Predictions. Part 1: Theory and Model Description. *Flow Turbulence and Combustion*, 85(1), pp.113-138.

Menter, F.R. & Kuntz, M., 2004. Adaptation of eddy-viscosity turbulence models to unsteady separated flow behind vehicles. *Symposium on "the aerodynamics of heavy vehicles: trucks, buses and trains." Monterey, USA, 2-6 Dec. 2002*.

Murthy, J.Y. et al., 2006. Survey of Numerical Methods. In W. J. Minkowycz, E. M. Sparrow, & J. Y. Murthy, eds. *Handbook of Numerical Heat Transfer*. pp. 1-984. Available at: http://onlinelibrary.wiley.com.sci-hub.org/book/10.1002/9780470172599.

OECD/NEA, 2011. *OECD/NEA: Report of the OECD/NEA-Vattenfall T-Junction Benchmark Excercise, Report No. NEA/CSNI/R(2011)-5*,

OECD/NEA, 2009. *OECD/NEA: T-Junction Benchmark Specifications, OECD/NEA & Vattenfall, Final Version*,

Odemark, Y. et al., 2009. High-Cycle Thermal Fatigue in Mixing Tees: New Large-Eddy Simiulations Validated Against New Data Obtained by PIV in the Vattenfall Experiment. In *Proceedings of the 17th International Conference on Nuclear Engineering*.

Ohtsuka, M. et al., 2003. LES analysis of fluid temperature fluctuations in a mixing Tee pipe with the same diameters. *ICONE 11-36064, 11th International Conference on Nuclear Engineering, Tokyo, Japan, April 20-23*.

Patankar, S.V., 1980. *Numerical Heat Transfer and Fluid Flow*,

Rhie, C.M. & Chow, W.L., 1983. Numerical Study of the Turbulent Flow Past an Airfoil with Trailing Edge Separation. *AIAA Journal*, 21(11), pp.1525–1532.

Shur, M.L. et al., 2008. A hybrid RANS-LES approach with delayed-DES and wall-modeled LES capabilities. *International Journal of Heat and Fluid Flow*, 29, pp.1638-1649.

Spalart, P.R., 2009. Detached eddy simulation. *Annu. Rev. Fluid Mech.*, 41, pp.181–202.

Spalart, P.R. et al., 2006. A new version of detached-eddy simulation, resistant to ambiguous grid densities. *Theor. Comput. Fluid Dyn.*, 20(3), pp.181-195.

Spalart, P.R. et al., 1997. Comments on the feaslibility of LES for wings, and on a hybrid RANS/LES approach. *Proceedings of first AFOSR international conference on DND/LES*, pp.1-11.

Strelets, M., 2001. Detached Eddy Simulation of Massively Separated Flows. *AIAA Paper*, 2001-0879, pp.1-18.